Physiologia Plantarum

An International Journal for Plant Biology

Physiologia Plantarum 167: 317–329. 2019

Acclimation and endogenous abscisic acid in the moss *Physcomitrella patens* during acquisition of desiccation tolerance

Kumudu N. Rathnayake[a], Sven Nelson[b], Candace Seeve[b], Melvin J. Oliver[b] and Karen L. Koster[a]*

[a]Department of Biology, University of South Dakota, Vermillion, SD, 57069, USA
[b]U.S. Department of Agriculture, Agricultural Research Service, Plant Genetics Research Unit, University of Missouri, Columbia, MO 65211, USA

Correspondence
*Corresponding author,
e-mail: karen.koster@usd.edu

Received 13 September 2018;
revised 26 November 2018

doi:10.1111/ppl.12892

The moss *Physcomitrella patens* has been used as a model organism to study the induction of desiccation tolerance (DT), but links between dehydration rate, the accumulation of endogenous abscisic acid (ABA) and DT remain unclear. In this study, we show that prolonged acclimation of *P. patens* at 89% relative humidity (RH) [−16 MPa] can induce tolerance of desiccation at 33% RH (−153 MPa) in both protonema and gametophore stages. During acclimation, significant endogenous ABA accumulation occurred after 1 day in gametophores and after 2 days in protonemata. *Physcomitrella patens* expressing the ABA-inducible EARLY METHIONINE promoter fused to a cyan fluorescent protein (CFP) reporter gene revealed a mostly uniform distribution of the CFP increasing throughout the tissues during acclimation. DT was measured by day 6 of acclimation in gametophores, but not until 9 days of acclimation for protonemata. These results suggest that endogenous ABA accumulating when moss cells experience moderate water loss requires sufficient time to induce the changes that permit cells to survive more severe desiccation. These results provide insight for ongoing studies of how acclimation induces metabolic changes to enable DT in *P. patens*.

Introduction

Desiccation tolerance (DT) has long been studied as a constitutive feature of many bryophytes, such as the moss *Syntrichia ruralis* (*Tortula ruralis*) (Bewley 1973, Bewley and Thorpe 1974). Recent analyses recognize that DT can also be induced in some bryophyte species previously considered to be desiccation-sensitive (Wood 2007, Stark 2017), including the model moss *Physcomitrella patens*. *Physcomitrella patens* has become a model for genomic, metabolic and proteomic studies because it has a sequenced genome, high efficiency of homologous recombination and a dominant haploid stage (Cove 2005, Cove et al. 2006). Early studies showed that *P. patens* could survive the loss of about 92% of its initial water content (WC), but not more extensive desiccation (Frank et al. 2005). This view was supported by a study demonstrating that *P. patens* survives moderate equilibrium drying to 91% relative humidity (RH; −13 MPa), but not rapid desiccation to

---

Abbreviations – ABA, abscisic acid; AMCYAN, *Anemonia majano* cyan; CTCF, corrected total cell fluorescence; DT, desiccation tolerance; dw, dry weight; EM, early methionine; hph, hygromycin B phosphotransferase gene; LEA, late embryogenesis abundant; RH, relative humidity; WC, water content.

water potentials below −13 MPa (Koster et al. 2010). In contrast, Wang et al. (2009) described *P. patens* as desiccation tolerant based upon recovery of growth after a one-month period of dehydration on agar.

Survival of desiccation depends on many factors, including drying rate (Proctor and Pence 2002, Stark 2017). Greenwood and Stark (2014) determined that slow drying over a 150-h period at high humidity could induce DT in gametophores of *P. patens*, as measured by improved survival and photosynthetic capacity. A recent study by Xiao et al. (2018) also demonstrated that gametophores, but not filamentous protonemata, can survive equilibration to water potentials below −100 MPa following a drying regime that features an initial phase with a slow rate of water loss.

The process of partial dehydration or hardening prior exposure to desiccating conditions can enhance or induce DT in plants (Proctor and Pence 2002, Wood 2007, Stark 2017). Previous studies reported that partial dehydration or hardening at high humidity can induce DT in the mosses *Atrichum androgynum* (Beckett 1999) and *Rhynchostegium riparioides* (Abel 1956). Partial dehydration or hardening has also been used to improve tolerance of rapid desiccation in plants that are already desiccation tolerant, including the moss *S. ruralis* (Schonbeck and Bewley 1981), the fern *Polypodium virginianum* (Bewley et al. 1993) and detached leaves of the angiosperm *Borya nitida* (Gaff and Churchill 1976).

Exogenous application of the phytohormone abscisic acid (ABA) can induce tolerance of rapid desiccation in *P. patens* protonemata (Oldenhof et al. 2006, Khandelwal et al. 2010, Koster et al. 2010, Pressel and Duckett 2010, Shinde et al. 2012) and gametophores (Koster et al. 2010), and endogenous ABA accumulation during dehydration has been reported in *P. patens* (Shinde et al. 2012, Xiao et al. 2018). However, some questions about the role of ABA in the induction of DT in *P. patens* remain. For example, Shinde et al. (2012) measured a rapid increase in the ABA content of protonemata during dehydration at 75% RH, but they did not report whether the moss survived the stress. Xiao et al. (2018) recently reported that although ABA accumulated during dehydration of *P. patens* gametophores and protonemata, elevated ABA amounts did not always correspond with DT in those tissues. Gametophores accumulated equal amounts of ABA during a gradual drying regime that led to DT and also during an equilibrium drying regime that did not induce DT, while protonemata accumulated significant amounts of ABA during gradual dehydration, but did not become desiccation tolerant (Xiao et al. 2018). It was suggested that factors in addition to ABA accumulation contribute to DT in *P. patens* and that the initial drying rate may be particularly important. Thus we initiated this study to further understand the link between ABA and acquisition of DT.

Another factor that could be important is the length of time between the accumulation of ABA and the loss of water needed to enable metabolic responses. Therefore, one aim of our study was to determine how the length of time allowed for the moss to respond to endogenous ABA influences the development of DT. A second aim was to examine the location of ABA accumulation in the tissues of *P. patens* as dehydration occurs in order to determine whether tissue-specific differences exist in the distribution of the phytohormone and whether these could account for reported differences in DT between gametophores and protonemata. Our results suggest that induction of DT in *P. patens* requires both ABA accumulation and sufficient time for tissues to respond with structural and metabolic changes and that ABA does not differentially accumulate between tissues.

Material and methods

Plant material and growth conditions

Physcomitrella patens (Hedw.) Bruch and Schimp., 'Gransden' ecotype, kindly provided by Dr Daniel Lynch (Williams College), was grown on 9-cm-diameter cellophane discs on top of solid BCDA medium as detailed by Cove et al. (2009). Cultures were maintained in a Percival 136-LLX (Perry, IA) growth chamber at 24°C with a 16/8-h light/dark cycle at 55–60 μmol m^{-2} s^{-1} light intensity. Samples were collected for protonema and gametophore acclimation experiments 3 and 5 weeks after subculturing, respectively.

Acclimation and desiccation protocols

Protonema- and gametophore-covered cellophane discs were cut into samples of approximately 2 × 2 cm using sterile scissors, and excess water was wiped from the moss surface using sterile Kim-wipe® tissue paper. Samples on cellophane were placed into aluminum weighing dishes (12-mm depth, 50-mm diameter) for ease of handling during acclimation and desiccation treatments. Moss samples were allowed to acclimate in sealed chambers over a saturated slurry of $MgSO_4$, which generates about 89% RH (−16 MPa) at 25°C (Winston and Bates 1960). This salt was chosen because it led to significant, but not lethal, dehydration in a prior study of *P. patens* (Koster et al. 2010). In that study, the temperature was 19°C, so the initial RH was slightly higher, at about 91%. RH was monitored using sensors (AcuRite 00325 W or SHT-31 probes, Sensirion Inc. with ±2% precision) in the chambers prior to and during each

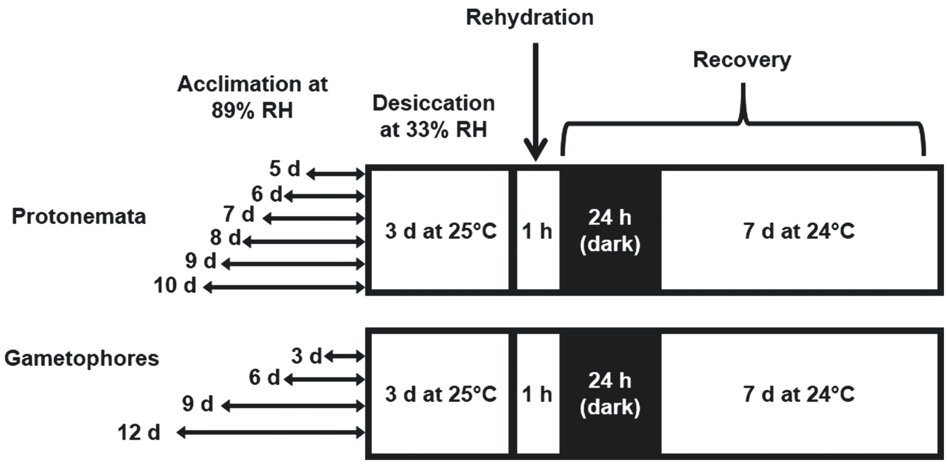

Fig. 1. Diagram of overall experimental design. Diagram represents acclimation at 89% RH (−16 MPa), desiccation at 33% RH (−153 MPa), rehydration, and the recovery period with assigned temperatures and the time periods for both protonemata and gametophores of *Physcomitrella patens*.

experiment. After acclimating for designated periods between 5 and 10 days for protonemata and 3 to 12 days for gametophores, samples were desiccated at 33% RH (−153 MPa) for an additional 3 days at 25°C (Fig. 1) in sealed chambers containing a saturated slurry of $MgCl_2$ (Rockland 1960). This salt was selected for desiccation because it dried the moss to WCs that did not differ from those attained by equilibration at 13% RH in the prior study (Koster et al. 2010), and there are fewer possible toxic effects of $MgCl_2$ than for the LiCl used before. Chambers for acclimation and desiccation were kept in a growth chamber at 25°C with a 16/8-h light/dark cycle at 55 to 60 μmol m^{-2} s^{-1} light intensity.

WC measurements

The WCs of four biological replicate samples were tracked throughout each acclimation and desiccation experiment. Four samples selected from those described above were transferred from cellophane to pre-weighed squares of aluminum foil, which do not hold water as the cellophane does and thus do not themselves lose water as the samples dehydrate, and weighed using a microbalance. These WC samples were placed in aluminum weighing dishes and randomly placed among the other samples in the chambers for acclimation at 89% RH. WC samples were weighed every 24 h until the end of the desiccation phase of the trial, oven dry weights (DWs) were measured after 48 h at 70°C. Weights of the aluminum foil squares were subtracted from all sample weights to obtain the weights of the moss. Drying curves plotting WC on a DW basis were generated by calculating the difference between the moss weight at each time (W_t) and the oven DW, divided by the oven DW as given in the following formula:

$$\mathrm{WC}\ \left(\mathrm{g\,g^{-1}\ dw}\right) = \left(W_t - \mathrm{DW}\right) / (\mathrm{DW})$$

Survival estimations

At the end of the 3-day desiccation period at 33% RH (−153 MPa), four biological replicates on cellophane were placed on two sterile, 9-cm diameter, Whatman #1 filter papers moistened with 3 to 4 ml of sterile water and allowed to slowly rehydrate for 1 h at 24°C. These samples were then transferred to solid BCDA medium and kept in darkness for 24 h at 24°C for further rehydration (Fig. 1). Following rehydration, samples were returned to the light conditions described above for acclimation for 7 days to observe if they maintained their green color and resumed growth.

Chlorophyll fluorescence measurements

Chlorophyll fluorescence of the rehydrated moss samples was measured using an Opti-Sciences modulated fluorometer model OS-100 (Hudson, NH, USA). Four biological replicates from each treatment were dark adapted for 10 min prior to measurements, and the F_v/F_m parameter was measured every 24 h for 3 days using a saturation pulse method as described by Maxwell and Johnson (2000). Chlorophyll fluorescence of four control samples that had not been dehydrated was also measured at each time point.

Endogenous ABA analysis

Samples were collected from four biological replicates for analysis of endogenous ABA at 24-h intervals during acclimation, and control samples collected prior to acclimation. Samples were flash frozen immediately in liquid nitrogen and ground to a fine powder using a pre-cooled mortar and pestle. Samples were lyophilized for 48 h prior to extraction. Endogenous ABA was extracted using the method in Yobi et al. (2017) with modifications as follow. For each replicate, 50 to 100 mg of lyophilized tissue was extracted using

1 ml of acidified 80% isopropanol (80:19:1, v/v/v, isopropanol/water/acetic acid) containing 6 ng ml^{-1} of (+)-*cis*,trans-ABA-d6 (d6-ABA) as the internal standard. The analysis was performed using an Agilent 1260 liquid chromatograph coupled with a single quadruple Mass Spectrometer equipped with electronic ionization mode as described by Xiao et al. (2018). In contrast to Xiao et al. (2018), where internal standard and endogenous ABA peaks were run in the same signal side-by-side, internal standard and endogenous ABA peaks were quantified from two independent signals during the same run to improve accuracy of quantification. Endogenous ABA concentrations for each sample were calculated using the slope of calibration curves constructed from peak area ratios of ABA to d6-ABA in a series of ABA:d6-ABA dilutions.

Plasmid construction

To characterize endogenous ABA localization during acclimation, a reporter construct consisting of an ABA-inducible wheat (*Triticum aestivum*) *EARLY METHIONINE* (*EM*) promoter (*PTaEM*) fused to a *CYAN FLUORESCENT PROTEIN* (*CFP*) reporter gene and Cauliflower mosaic virus (*CaMV*) *35*$_{s}$ terminator was used. The *EM* promoter has previously been used to measure ABA responses in *P. patens* (Knight et al. 1995). This ABA-regulated CFP reporter construct was derived from a *PTaEM::GUS::35*$_{s}$ construct that had been cloned into the pGEM®-3Z vector (Promega, Madison, WI) and was kindly provided by Pierre-François Perroud and Ralph Quatrano (Washington University). The *PTaEM::GUS::35*$_{s}$ cassette was amplified with M13-F1(−40) and M13-R1 primers (Table S1) and was cloned into the pCR®8/GW/TOPO vector (Invitrogen by Thermo Fisher Scientific, Carlsbad, CA). The *PTaEM* was amplified with the GW1-F1 primer and the *EMBam*HI-R1 primer (Table S1) to incorporate the *Bam*HI restriction site to the 3′ end of the promoter. The *Anemonia majano* cyan (*AMCYAN*) gene in the pAmCyan vector (Clontech Laboratories, Mountain View, CA) was amplified with the primers Cyan-F1 and Cyan*Pst*I-R1 (Table S1) to incorporate the *Pst*I site to the 3′ end of the gene. Amplified *PTaEM* and *AMCYAN* genes were digested with restriction enzymes *Hind*III and *Bam*HI, and *Bam*HI and *Pst*I, respectively. Appropriate bands were cut after digestion and were ligated to the pCR®8/GW vector, which had been digested with *Hind*III and *Pst*I restriction enzymes to remove *PTaEM::GUS*. The sequence of *PTaEM::CFP::35*$_{s}$ was verified by Sanger sequencing. The *PTaEM::CFP::35*$_{s}$ in pCR®8/GW vector was used as an entry vector for LR Clonase™ reaction (Invitrogen, Carlsbad, CA) to transfer the cassette into the plant expression vector, xk2, between the *P. patens* Pp108 locus homologous recombination flanking regions and which contains the *HYGROMYCIN B PHOSPHOTRANSFERASE* gene (*HPH*) for selection.

Protoplast transformation and selection of transgenic lines

Protoplasts isolated from 5-day-old *P. patens* protonemata were transformed with linearized *PTaEM::CFP::35s* plasmids using polyethylene glycol-mediated transformation (Roberts et al. 2011). Briefly, 5 days after transformation, first round selection was performed using 25μg ml^{-1} hygromycin B incorporated into solid BCDA. After 7 days on selection medium, colonies were transferred to BCDA medium for 1 week and subsequently back to selection medium for a week. Two stable transgenic lines survived after the second round of selection. Integration of the *PTaEM::CFP::35s* DNA cassette into the Pp108 locus of the genome by homologous recombination was confirmed by polymerase chain reaction using the *Pp*1085′-F1 primer specific to the genomic region flanking the homologous region and 35shphCaMV-R1 primer which primes within the donor cassette (Table S1).

Confocal imaging

Both protonemata and gametophores of the *PTaEM*:*CFP* T1 line were subjected to acclimation at 89% RH (−16 MPa); samples were collected throughout the course of acclimation as described above. Acclimated protonemata and gametophores were rehydrated on moistened Whatman #1 filter paper approximately 1 to 2 h before imaging with a 40× water objective on a Leica TCP SP8 laser scanning confocal microscope equipped with fixed argon laser lines and a tunable super continuum white light laser. CFP was excited at 458 nm by the argon laser line and the emission bandpass was 465–520 nm. Samples of the *PTaEM*:*CFP* line treated with 50μM ABA for 48 h were used as positive controls, and untransformed *P. patens* (both with and without ABA treatment) were used as negative controls. Fiji software (Schindelin et al. 2012) was used to analyze the corrected total cell fluorescence (CTCF) intensities of unprocessed images as explained by McCloy et al. (2014). All images collected from confocal microscopy to be used in figures were then processed for brightness and contrast using Adobe Photoshop CC 2017.

Statistical analysis

Data were statistically analyzed using IBM®SPSS® V25 software. One-way ANOVA was performed followed by comparison of means using Tukey's test ($P < 0.05$) for endogenous ABA data and CTCF data. Student's *t*-test was used to the compare the significant differences ($P < 0.05$) of the survival among treatments.

Results

Survival and WC of the acclimated moss

Protonema samples that acclimated for 5 to 8 days did not survive desiccation upon rehydration and became completely chlorotic after 3-day recovery on the BCDA medium (Fig. S1). However, protonema samples that acclimated for 9 and 10 days at 89% RH (−16 MPa) stayed green after rehydration and started re-growth on BCDA medium during the recovery period (Fig. S1). Protonemata lost water gradually during the acclimation period at 89% RH and further desiccated during 3 days at 33% RH (−153 MPa). Average WCs at the end of the acclimation at 89% RH and at the end of 33% RH desiccation for protonemata were 0.59 ± 0.042 and 0.12 ± 0.063 g g^{-1} dw, respectively (Fig. 2A).

Gametophores acclimated for 6, 9 or 12 days survived desiccation at 33% RH and remained green after rehydration, while samples acclimated for 3 days did not recover after desiccation and rehydration (Fig. S2). The average WC of the gametophores at the end of acclimation (89% RH) was 0.57 ± 0.039 g g^{-1} dw and at the end of desiccation (33% RH) was 0.06 ± 0.012 g g^{-1} dw (Fig. 2B).

Chlorophyll fluorescence

The F_v/F_m ratio, an indicator of Photosystem II (PSII) efficiency, was measured for both protonemata and gametophores upon rehydration. The chlorophyll fluorescence of protonema samples that acclimated for 5 to 8 days declined over the course of the first 72 h of recovery (following rehydration), while 9 and 10 days acclimated samples showed gradual increases in chlorophyll fluorescence (Fig. 3A). In gametophores, the F_v/F_m values of 3-day-acclimated samples gradually decreased during the first 72 h of recovery after rehydration. In contrast, 6, 9 and 12 days acclimated gametophores showed increased F_v/F_m values (Fig. 3B), indicating recovery of photosynthetic capacity in PSII. Survival percentages of each treatment were also quantified by comparing the maximum quantum efficiency (F_v/F_m) of each sample after 72-h recovery period to the F_v/F_m ratio of unstressed controls of the same age. Using this measure of survival, the 9 and 10 days acclimated protonema samples had survival percentages above 70% (Fig. 4A), while gametophore DT was maximal after 6 days of acclimation (Fig. 4B). Survival percentage of 6 days acclimated gametophores were significantly different from 9 and 12 days acclimated gametophores (Fig. 4B). The F_v/F_m ratio of gametophores acclimated for longer periods (9 and 12 days) did not recover to the same level as undried controls, although recovery to levels above 50% of the initial value were measured (Fig. 4B).

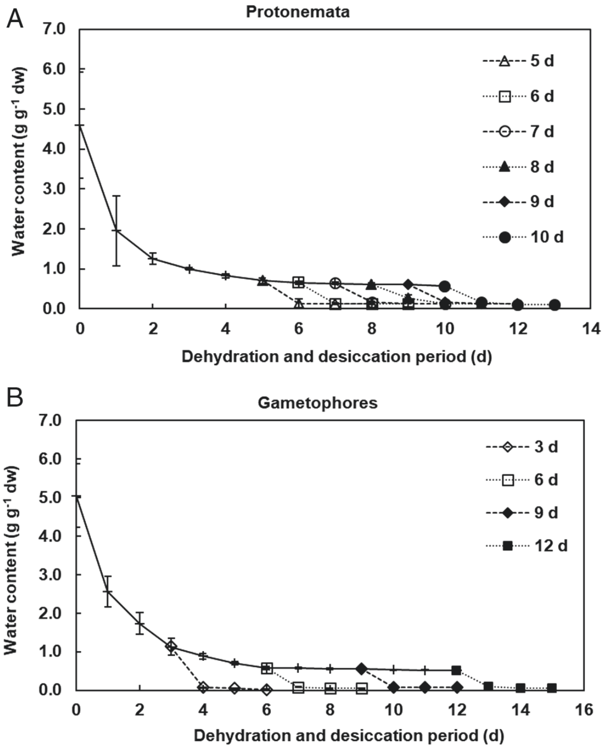

Fig. 2. WC of *Physcomitrella patens* during acclimation and desiccation on dw basis. Drying curves of (A) protonemata and (B) gametophores show the gradual decrease of WC during acclimation at 89% RH (−16 MPa) and additional drop in WC when samples were desiccated at 33% RH (−153 MPa) beginning on the days indicated. Data shown are means ± SD of pooled replicate moss samples, where eight samples were removed from the total pool and desiccated at each indicated time. For protonemata, n = 48 samples in the total pool, and for gametophores, n = 32 samples. Error bars are not visible when they are smaller than the symbol.

Accumulation of endogenous ABA

Endogenous ABA accumulated to concentrations significantly greater than in unstressed controls ($P < 0.05$) after 3 days of acclimation for protonemata and after 1 day of acclimation for gametophores (Fig. 5A, B). After 9 and 10 days of acclimation of protonemata, ABA amounts increased by ninefold compared to unstressed protonemata; endogenous ABA concentrations were also significantly ($P < 0.05$) higher in 9 and 10 days acclimated protonemata than in all other time points (Fig. 5A). In gametophores, the endogenous ABA concentration

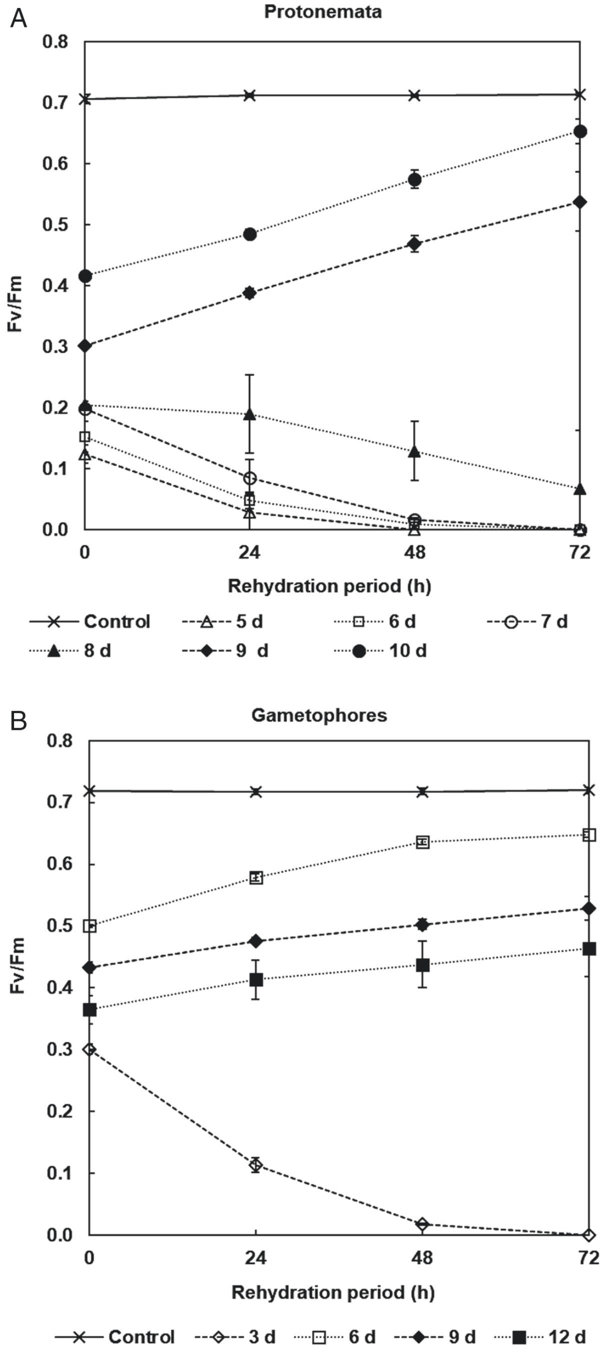

Fig. 3. Changes in F_v/F_m parameter during recovery. F_v/F_m ratio changes in (A) protonemata and (B) gametophores during 72-h rehydration on BCDA medium. Data shown are means ± SD of eight replicates for each developmental stage. Error bars are not visible when they are smaller than the symbol.

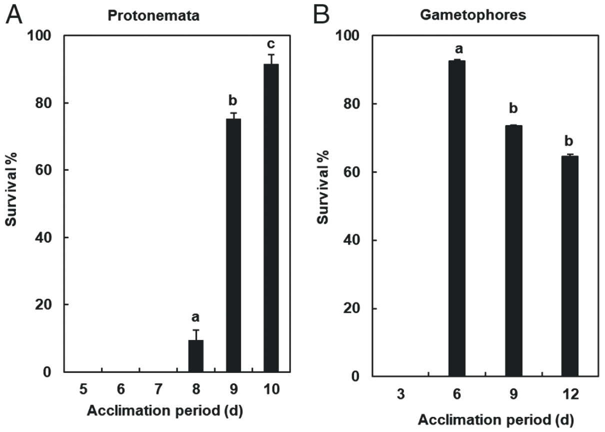

Fig. 4. Survival percentages of moss after rehydration. Survival percentages were calculated as the chlorophyll F_v/F_m ratio of the recovered sample after 72-h rehydration compared to the F_v/F_m ratio of unstressed controls of the same age. Each bar shows the mean of eight biological replicates (mean ± SD) of (A) protonemata and (B) gametophores. Each set of moss samples was first acclimated for the designed acclimation period at 89% RH and desiccated at 33% RH for 3 days. In each graph, bars labeled with the same letters are not significantly different ($P < 0.05$), while different letters above bars indicate significant differences among results.

reached a maximum concentration of 1119 ± 39 ng g^{-1} dw after 12 days of acclimation (Fig. 5B). The maximum concentration of ABA accumulated in protonemata was 6022 ± 308 ng g^{-1} dw, which was significantly ($P < 0.05$) higher than in gametophores.

Endogenous ABA localization in moss during acclimation

To investigate the localization of endogenous ABA production during acclimation, moss was transformed with *PTaEM::CFP::35s* cassette (Fig. S3). The construct was targeted for homologous recombination into the Pp108 gene in the genome as described by Schaefer and Zrÿd (1997). After two rounds of selection with hygromycin B, two stable transgenic lines were isolated (*PTaEM::CFP* T1 and T2). The expected ≈2.5-kb band in Fig. S4 confirmed the integration of *PTaEM::CFP::35s* DNA fragment into the moss genome. The *PTaEM::CFP* T1 line was chosen for further study because it had greater intensity of the ≈2.5-kb band and, on preliminary examination with confocal microscopy of ABA-treated samples, it exhibited the strongest fluorescence intensity.

Confocal microscopy observations of the *PTaEM::CFP* T1 transgenic line revealed CFP signal in the cytoplasm of cells of both developmental stages of *P. patens*. Moss cells lost some water during acclimation, leading to flattening and twisting of protonemal filaments; cytoplasm of the cells was concentrated either to the middle of the

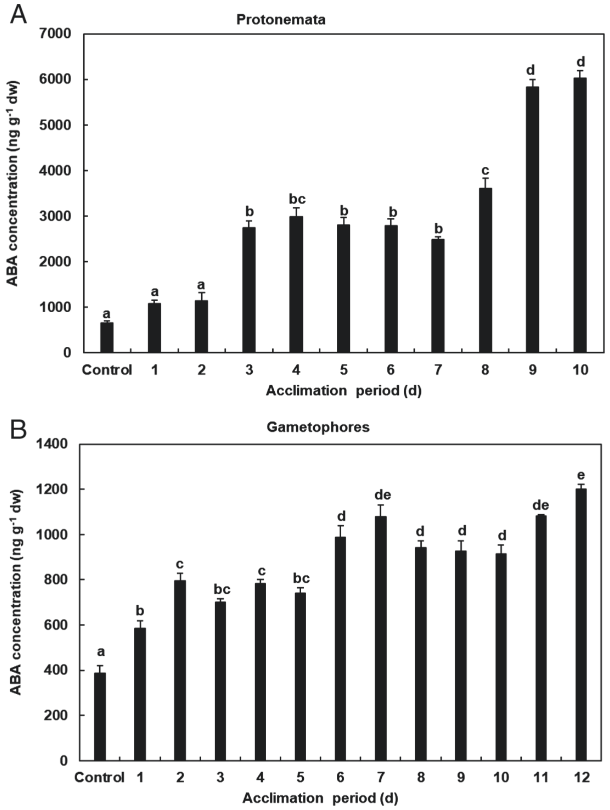

Fig. 5. Endogenous ABA concentration changes on a dw basis during acclimation. Endogenous ABA accumulation in (A) protonemata and (B) gametophores that were subjected to acclimation at 89% RH (−16 MPa) for 1 to 10 days and 1 to 12 days, respectively. Data shown are means ± SD of three replicates for each developmental stage of the moss including non-acclimated controls. In each graph, bars labeled with the same letters are not significantly different ($P < 0.05$), while different letters above bars indicate significant differences among results.

cell or to the ends near the transverse walls (Fig. S5). Upon rehydration, cells in all treatments regained their original shapes although plastids were scattered in the cytoplasm of the cells (Fig. 6). Many small vesicles were present in the chloronemal cells of 2- to 10-day acclimated protonemata after rehydration (Fig. 6). However, those small vesicles were not detected in chloronemal cells of the ABA-treated T1 line nor in non-transformed wild-type controls, neither of which had been acclimated and thus dehydrated (Fig. 6). The CFP signal increased in protonema cells during the acclimation period, indicating accumulation of endogenous ABA in chloronemal cells (Fig. 7A). Protonemata acclimated for 9 and 10 days had significantly greater ($P < 0.05$) CTCF intensities than 1 to 8 days acclimated protonemata.

After 1 to 2h rehydration on the filter papers, visual evidence shows that most of the cells in the leaf-like phyllids of 2 to 10 days acclimated gametophores had intact plasma membranes with scattered ovoid plastids (Fig. 8). A few dead cells without contents were seen in phyllids of 10 days acclimated gametophores (Fig. 8). Gametophore samples acclimated for 1 to 3 days showed low CTCF intensities after rehydration (Figs 7B, 8), indicating low concentrations of endogenous ABA had accumulated in the cells during this period. Further acclimation for 7 to 10 days increased the CFP fluorescence intensity (Figs 7B and 8), and 7 and 8 days acclimated samples had significantly ($P < 0.05$) higher CTCF intensities compared to 1 to 3 days acclimated moss. The CTCF intensity data align with the endogenous ABA concentrations measured using LC–MS for acclimated protonemata and gametophores.

Based on our sample size, CFP intensities did not appear to differ systematically among cell types with the exception of gametophore buds. Fig. S6A shows that apical cells in the lower level of the buds with leaf primordia had strong CFP signals even by 3 days of acclimation, whereas CFP was absent in the rest of the bud during the early stage of the acclimation. Over the time of acclimation, the CFP signal slowly accumulated throughout the bud; however, the intensities remained lower than those in the apical stem cells at the base of the bud (Fig. S6B).

Discussion

Bryophytes vary in their ability to tolerate desiccation. Some mosses, such as *S. ruralis*, have constitutive DT with cellular protection mechanisms that appear to be independent of ABA signaling; they can survive rapid dehydration without priming (Bewley et al. 1993). Others have inducible DT that depends on factors such as the drying rate, period of exposure to desiccation, extent of desiccation and the rate of rehydration (Bewley 1979, Proctor and Pence 2002, Stark 2017). *Physcomitrella patens* is classified as inducibly desiccation tolerant, as exogenous ABA induces DT in protonemata (Oldenhof et al. 2006) and gametophores (Koster et al. 2010). Recent studies have also shown that very slow dehydration of *P. patens* gametophores, but not protonemata, can induce DT (Greenwood and Stark 2014, Xiao et al. 2018).

The results of this study demonstrate that *P. patens* protonemata can also become desiccation tolerant if they acclimate during non-lethal dehydration [89% RH (−16 MPa)] for a prolonged period of 9 to 10 days prior to desiccation. Both the drying rate and the length of acclimation were important factors in the acquisition of DT. During acclimation, protonemata required 120 h (5 days) to achieve a constant weight at 89% RH (Fig. 2A), and further 3 days were needed for DT to

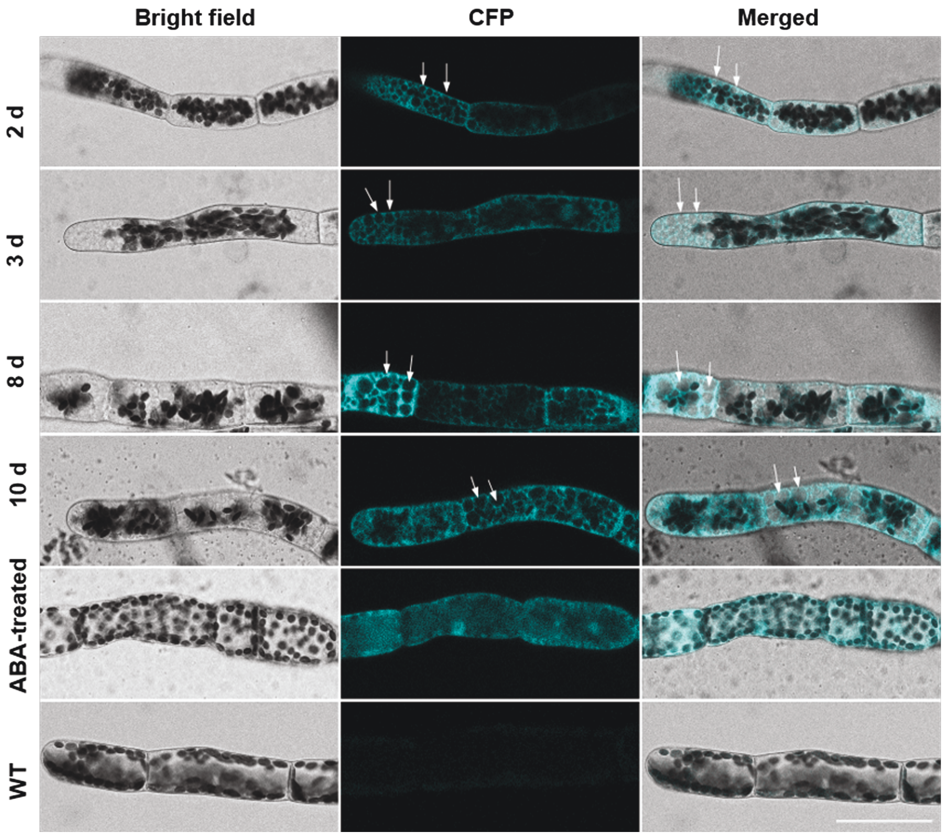

Fig. 6. CFP localization in acclimated protonemata. Protonemata were allowed to acclimate for periods indicated to the left of each row, prior to rehydration for 1 to 2 h and imaging using confocal microscopy. Brightfield images of chloronema cells are shown with their corresponding CFP signal and merged images. Note numerous cytoplasmic vesicles (arrows) in cells of moss exposed to 89% RH (−16 MPa). ABA-treated moss (positive control) and wild-type (negative control) lacked similar vesicles. No CFP signal was detected in the WT controls. All pictures were taken using a 40× objective. Scale bar represents 25 μm.

develop (Fig. 2A). The equilibrium WCs reported here at 89% RH are slightly higher than those reported by Koster et al. (2010) for mixed protonemata and gametophores at 91% RH (0.32 g g^{-1} dw), which may be a result of the smaller sample sizes used in the earlier study. The very slow drying rate measured here is slower than that reported for protonemata by Xiao et al. (2018). In that study, protonemata reached equilibrium with 50% RH (−100 MPa) after 96 h (4 days) and did not survive the desiccation. We hypothesize that the very slow dehydration phase in the current study triggered the induction of DT in protonemata, with the extended acclimation period enabling the cells to mobilize protective metabolites and proteins.

Induction of DT typically involves signaling by ABA (Marella et al. 2006, Khandelwal et al. 2010), although ABA-independent pathways are also known (Shinozaki and Yamaguchi-Shinozaki 1997) and have been implicated in responses of *P. patens* to dehydration (Cuming et al. 2007). During the first 3 days of acclimation, endogenous ABA in the protonemata rose to about 3000 ng g^{-1} dw, concentrations approximately fourfold greater than those measured in the control. ABA concentrations were then constant from day 3 through day 8, after which they rose further to about nine times the concentration in control protonemata tissues (Fig. 4A). Xiao et al. (2018) also reported a significant increase in ABA to about 400 ng g^{-1} dw in gradually dried protonemata, although in that case, the tissue did not survive desiccation, either because insufficient ABA accumulated or because there was insufficient time to respond to the ABA before desiccation. In general, the amounts of ABA we report here are considerably higher than those reported in the previous work by Xiao et al. (2018). The discrepancy may lie in part from the 2 to 5 times larger sample sizes used in the current study, which improves the accuracy of detection by the LC–MS. The improvement in the internal standard methodology (described in materials and methods) that improved accuracy of the quantification may also explain the discrepancy.

Our gametophore survival results are supported by the Greenwood and Stark (2014) study showing some gametophore survival to water potentials below −100 MPa after slow dehydration to 30 or 50% RH. Water added to the samples before dehydration in that study resulted in the elevation of the ambient RH to 95% for approximately the first 175 h of dehydration, after which the samples dried rapidly. Greenwood and Stark (2014) hypothesized that the prolonged drying rate induced DT, and Xiao et al. (2018) supported this by showing that very

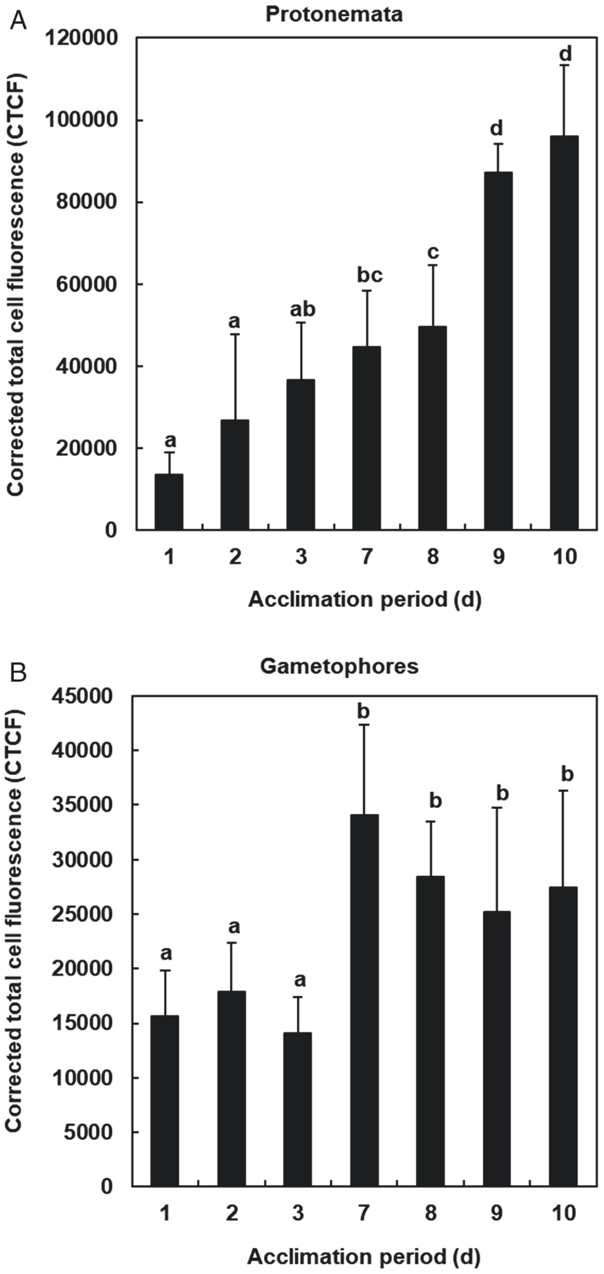

Fig. 7. Quantitative analysis of CFP signal in acclimated moss. CFP intensities in acclimated (A) protonemata and (B) gametophores were calculated as CTCF using Fiji image analysis software for randomly selected cells (n = 10) in each sample. In each graph, bars labeled with the same letters are not significantly different ($P < 0.05$), while different letters above bars indicate significant differences among results. Data shown are means ± SD of 10 cells for each treatment.

slow drying regimes could induce DT in *P. patens* gametophores. Xiao et al. (2018) also demonstrated that ABA accumulated to high concentrations in dehydrating tissue; however, ABA accumulation did not always correlate with DT. ABA concentrations in gametophores that dried gradually over 5 days were similar to the concentrations of ABA found in tissue that had been dried quickly, and then held at 90% RH for 3 to 5 days. However, only gradually dried gametophores survived subsequent desiccation (Xiao et al. 2018). Similarly, we show here that 3 days of acclimation at 89% RH did not induce DT, but 6 days of acclimation led to almost complete DT, as quantified by recovery of photosynthetic efficiency (F_v/F_m) and maintenance of green color (Figs 4B and S3).

In this study, ABA concentrations in both protonemata and gametophores increased throughout the acclimation period (Fig. 5A, B), and it is possible that the high concentrations of ABA accumulating during the initial days of acclimation were not sufficient to reach a threshold for response. Given the relatively high amounts of ABA detected here during the early stages of acclimation compared to the amounts reported to induce DT elsewhere (e.g. Shinde et al. 2012, Xiao et al. 2018), we think this possibility is less likely than a requirement for sufficient time to respond. We also note that significantly higher amounts of ABA were measured in desiccation tolerant protonemata compared to desiccation tolerant gametophores, suggesting that the two tissues might have different thresholds for response to the same stress. This idea is supported by Zhang et al. (2015) who showed that expression levels of nuclear factor YC5 (*PpNF-YC5*), which acts synergistically with ABI3 in regulation of ABA responses (Yotsui et al. 2013), differed widely among *P. patens* developmental stages, with unstressed gametophores having from 6- to 120-fold the amounts detected in protonemata. Perhaps this suggests that gametophores are already primed to respond to dehydration, while protonemata require additional ABA or time to respond, or perhaps it reflects developmental differences in the sensitivity to the hormone.

ABA acts as a signaling molecule to activate stress-responsive genes and protective proteins, including some late embryogenesis abundant (LEA) proteins, in vegetative tissues and seeds of different plant species (Lane 1991, Berjak et al. 2007, Shinde et al. 2013). ABA biosynthesis and some key signaling core components such as *ABI3* and *ABI1* are well characterized in *P. patens* (Marella et al. 2006, Komatsu et al. 2009, Takezawa et al. 2015). Proteomic (Wang et al. 2010, Wang et al. 2012) and genomic (Cuming et al. 2007, Richardt et al. 2010) studies showed that application of exogenous ABA could activate ABA-responsive genes and initiate the production of some LEA proteins and heat shock proteins presumed to protect *P. patens* cells during desiccation. Thus, endogenous ABA accumulating early during acclimation could trigger ABA-responsive genes and the synthesis of protective proteins and thereby limit cellular damage when desiccation occurs.

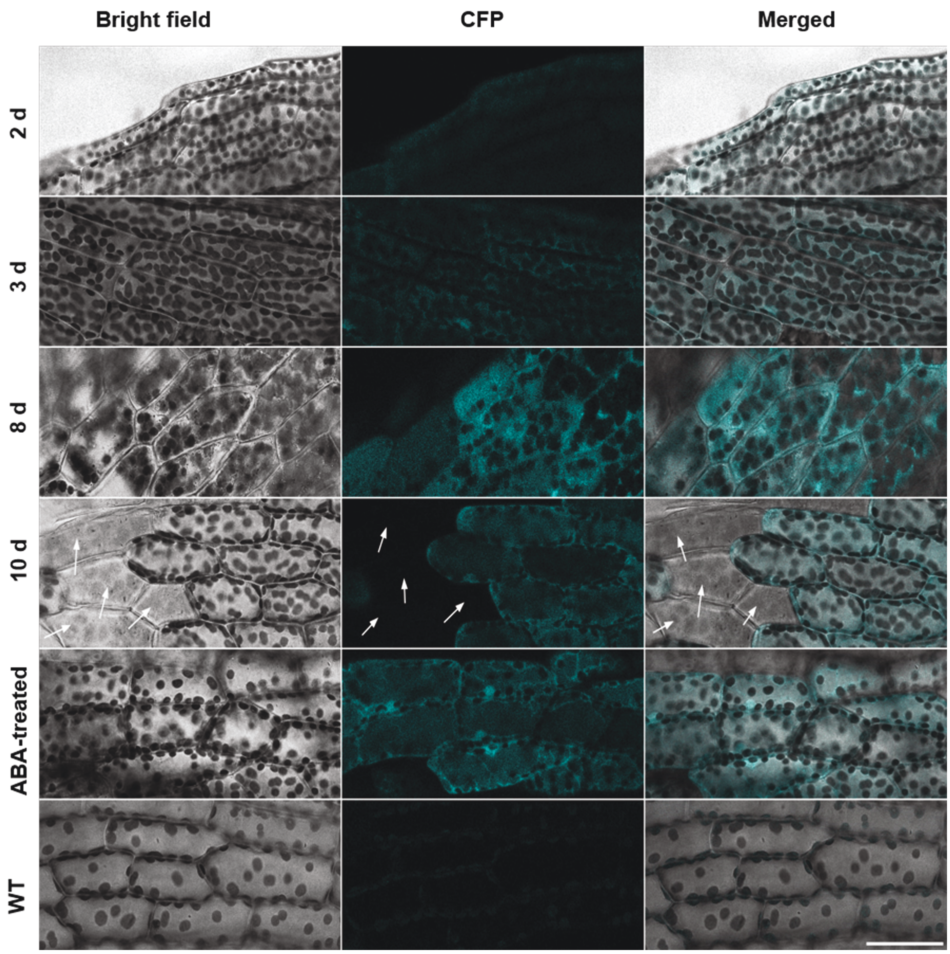

Fig. 8. CFP localization in acclimated gametophores. Brightfield images of rehydrated cells on leaf-like phyllids of gametophores after certain acclimation period with their corresponding CFP signal are indicated along with merged images. Arrows indicate dead cells on phyllids of gametophores after rehydration. ABA-treated moss was used as the positive control and wild type used as the negative control, which had only the autofluorescence for plastids. All pictures were taken using 40× objective. Scale bar represents 25 μm.

The lengthy time required for the ABA response during acclimation in this study may be a result of increased cellular viscosity and slowed metabolism in the moss cells at the lowered WC (approximately 0.58 g g^{-1} dw, Fig. 2). As cells dehydrate, cytoplasmic viscosity increases (Leprince and Hoekstra 1998), and thus metabolism either slows down or occurs at a minimal level. Leprince and Hoekstra (1998) showed that cytoplasmic viscosity increased exponentially in dehydrated cowpea (*Vigna unguiculata*) cotyledons and *Typha latifolia* pollen when WC fell below about 0.8 g g^{-1} dw. Respiratory O_2 and CO_2 exchange slowed steadily as the cells dried, and reached about 50% of the fully hydrated value as at WCs around 0.6 g g^{-1} dw (Leprince and Hoekstra 1998). A similar slowing of respiratory O_2 uptake was measured by Bewley and Thorpe in the moss *S. ruralis* at WCs 31to 36% fresh weight (Bewley and Thorpe 1974). Therefore, we speculate that the accumulation of protective proteins and metabolites may take longer periods to reach sufficient abundance at low WCs compared to hydrated cells. However, further investigation is necessary to understand how prolonged acclimation alters metabolic responses in *P. patens* to minimize the damage that could occur during desiccation and rehydration.

Increased chlorophyll fluorescence (F_v/F_m) ratios measured in 9 to 10 days acclimated protonemata and 6 days acclimated gametophores upon rehydration indicate that acclimation minimizes the PSII damage that otherwise occurs during desiccation or rehydration (Fig. 3A, B). However, recovery was slow: F_v/F_m ratios increased by only 0.1 during the first 24 h and had not reached control levels in most treatment during 3 days of recovery in protonemata (Fig. 3A). In contrast to the slow recovery of PSII measured in our study, the moss *A. androgynum*, when pre-treated with exogenous ABA had a rapid recovery of PSII efficiency within 8 h of rehydration following desiccation over silica gel (Mayaba et al. 2001). Mayaba et al. (2001) further reported rapid recovery of respiratory activity and increased non-photochemical quenching in the ABA-treated *A. androgynum*. Air-dried, desiccation tolerant *Anomodon viticulosus*, also showed a rapid recovery of PSII in less than an hour (Proctor and Smirnoff 2000). The slower recovery of PSII measured in acclimated desiccation tolerant *P. patens* suggests that acclimation might activate different metabolic pathways compared to the mechanisms present in constitutively desiccation tolerant moss or DT induced by exogenous ABA.

Constitutively DT organisms divert energy from reproduction and growth to maintain the protective mechanisms required for DT (Toldi et al. 2009). Inducible DT in *P. patens* has both advantages and disadvantages: while energy is not continually diverted from growth and reproduction, *P. patens* cannot survive rapid desiccation because sudden desiccation stress does not give enough time to induce DT. Although most cells in a *P. patens* plant do not survive rapid desiccation, a few cells often do remain green and gradually regenerate a colony (Koster et al. 2010). One possible explanation for this is that some cells respond more quickly to water loss by producing ABA and so can prime themselves to survive desiccation. Understanding the localization of endogenous ABA in different cell types of *P. patens* during acclimation might indicate whether some cell types will survive desiccation better than others. Our observations of a transgenic ABA-reporter line during acclimation did not reveal a difference between the distribution of ABA in different cell types with the exception of buds. In buds, high concentrations of the CFP signal were observed early during acclimation, but only in the apical stem cells at the base of the gametophore buds (Fig. S6A). The CFP signal was absent in the early stages of acclimation in leafy buds, although it gradually accumulated there at the later stages of acclimation (Fig. S6B). Fluorescence intensities were higher in protonemata than in gametophores, in accord with the differences in ABA measured between the two tissues (Fig. 5). Overall, our observations indicate that most of the cell types in *P. patens* accumulate endogenous ABA in response to dehydration. The structural changes observed in cells during acclimation, such as flattening and twisting of the protonemata (Fig. S5), appear to be reversible after rehydration (Fig. 6). Furthermore, the small vesicles observed in the chloronemal cells are likely to fuse to form larger vacuoles during recovery after rehydration. Pressel and Duckett (2010) reported a similar pattern of vesicle formation in slowly dehydrated protonema cells after rehydration, as well as fusion of those vesicles over several hours of rehydration indicating recovery of cells.

Our study demonstrates that *P. patens* can acquire DT to water potentials below −150 MPa in both protonemata and gametophores if cells acclimate for a prolonged period at high humidity prior to desiccation. Furthermore, we conclude that in addition to a slow initial drying rate to trigger acclimation, the length of the acclimation period and endogenous ABA accumulation are both important factors for the development of DT in *P. patens*. Furthermore, we hypothesize that endogenous ABA accumulating early in acclimation triggers production of protective metabolites and proteins that accumulate and minimize desiccation damage. Further research will investigate how metabolic pathway alterations during acclimation contribute to DT in *P. patens*.

Author contributions

K.N.R. designed and conducted the experiments, interpreted results and wrote the manuscript. S.N. supervised and assisted measurements of endogenous ABA. C.S. constructed the *PTaEM::CFP::35s* DNA cassette. M.J.O. assisted with experimental design, supervision of ABA measurements and data interpretation. K.L.K. conceptualized, supervised all work, assisted with data interpretation and revised the manuscript. All authors read and approved the manuscript.

Acknowledgements – We thank Dr. Frank Baker of Molecular Cytology Core in University of Missouri for his assistance with confocal microscopy and Jim Elder of the USDA-ARS for lab support. This work was supported by the University of South Dakota (USD) graduate research and creative scholarship grants to K.N.R., by the USD Department of Biology, and by the National Science Foundation Collaborative Research: Dimensions: Grant Number 1638972 to M.J.O. Mention of trademark or proprietary product does not constitute a guarantee or warranty of the product by the U.S. Department of Agriculture and does not imply its approval to the exclusion of other products that may be suitable.

References

Abel WO (1956) Die austrocknungsresistenz der laubmoose. Sitzungsberichte, Vol. 165. Österr Akad Wiss, Math-nat Kl, pp 619–707

Beckett RP (1999) Partial dehydration and ABA induce tolerance to desiccation-induced ion leakage in the moss *Atrichum androgynum*. S Afr J Bot 65: 212–217

Berjak P, Farrant JM, Pammenter NW (2007) Seed desiccation-tolerance mechanisms. In: Jenks MA, Wood AJ (eds) Plant Desiccation Tolerance. Blackwell Publishing, CAB International Press, Wallingford, pp 149–192

Bewley JD (1973) Desiccation and protein synthesis in the moss *Tortilla ruralis*. Can J Bot 51: 203–206

Bewley JD (1979) Physiological aspects of desiccation tolerance. Annu Rev Plant Physiol 30: 195–238

Bewley JD, Reynolds TL, Oliver MJ (1993) Evolving strategies in the adaptation to desiccation. In: Close TJ, Bray EA (eds) Plant Responses to Cellular Dehydration

During Environmental Stress. American Society of Plant Physiologists, Rockville, MD

Bewley JD, Thorpe TA (1974) On the metabolism of *Tortula ruralis* following desiccation and freezing: respiration and carbohydrate oxidation. Physiol Plant 32: 147–153

Cove D (2005) The moss *Physcomitrella patens*. Annu Rev Genet 39: 339–358

Cove D, Bezanilla M, Harries P, Quatrano R (2006) Mosses as model systems for the study of metabolism and development. Annu Rev Plant Biol 57: 497–520

Cove DJ, Perroud P-F, Charron AJ, McDaniel SF, Khandelwal A, Quatrano RS (2009) Culturing the moss *Physcomitrella patens*. Cold Spring Harb Protoc 2009. https://doi.org/10.1101/pdb.emo115

Cuming AC, Cho SH, Kamisugi Y, Graham H, Quatrano RS (2007) Microarray analysis of transcriptional responses to abscisic acid and osmotic, salt, and drought stress in the moss, *Physcomitrella patens*. New Phytol 176: 275–287

Frank W, Ratnadewi D, Reski R (2005) *Physcomitrella patens* is highly tolerant against drought, salt and osmotic stress. Planta 220: 384–394

Gaff D, Churchill D (1976) *Borya nitida* Labill-an Australian species in the Liliaceae with desiccation-tolerant leaves. Aust J Bot 24: 209–224

Greenwood JL, Stark LR (2014) The rate of drying determines the extent of desiccation tolerance in *Physcomitrella patens*. Funct Plant Biol 41: 460–467

Khandelwal A, Cho SH, Marella H, Sakata Y, Perroud PF, Pan A, Quatrano RS (2010) Role of ABA and ABI3 in desiccation tolerance. Science 327: 546

Knight CD, Sehgal A, Atwal K, Wallace JC, Cove DJ, Coates D, Quatrano RS, Bahadur S, Stockley PG, Cuming AC (1995) Molecular responses to abscisic acid and stress are conserved between moss and cereals. Plant Cell 7: 499–506

Kofuji R, Hasebe M (2014) Eight types of stem cells in the life cycle of the moss *Physcomitrella patens*. Curr Opin Plant Biol 17: 13–21

Komatsu K, Nishikawa Y, Ohtsuka T, Taji T, Quatrano RS, Tanaka S, Sakata Y (2009) Functional analyses of the ABI1-related protein phosphatase type 2C reveal evolutionarily conserved regulation of abscisic acid signaling between *Arabidopsis* and the moss *Physcomitrella patens*. Plant Mol Biol 70: 327–340

Koster KL, Balsamo RA, Espinoza C, Oliver MJ (2010) Desiccation sensitivity and tolerance in the moss *Physcomitrella patens*: assessing limits and damage. Plant Growth Regul 62: 293–302

Lane BG (1991) Cellular desiccation and hydration: developmentally regulated proteins, and the maturation and germination of seed embryos. FASEB J 5: 2893–2901

Leprince O, Hoekstra FA (1998) The responses of cytochrome redox state and energy metabolism to dehydration support a role for cytoplasmic viscosity in desiccation tolerance. Plant Physiol 118: 1253–1264

Marella HH, Sakata Y, Quatrano RS (2006) Characterization and functional analysis of ABSCISIC ACID INSENSITIVE3-like genes from *Physcomitrella patens*. Plant J 46: 1032–1044

Maxwell K, Johnson GN (2000) Chlorophyll fluorescence-a practical guide. J Exp Bot 51: 659–668

Mayaba N, Beckett RP, Csintalan Z, Tuba Z (2001) ABA increases the desiccation tolerance of photosynthesis in the afromontane understorey moss *Atrichum androgynum*. Ann Bot 88: 1093–1100

McCloy RA, Rogers S, Caldon CE, Lorca T, Castro A, Burgess A (2014) Partial inhibition of Cdk1 in G 2 phase overrides the SAC and decouples mitotic events. Cell Cycle 13: 1400–1412

Oldenhof H, Wolkers WF, Bowman JL, Tablin F, Crowe JH (2006) Freezing and desiccation tolerance in the moss *Physcomitrella patens*: an in situ Fourier transform infrared spectroscopic study. Biochim Biophys Acta 1760: 1226–1234

Pressel S, Duckett JG (2010) Cytological insights into the desiccation biology of a model system: Moss protonemata. New Phytol 185: 944–963

Proctor MC, Pence VC (2002) Vegetative tissues: bryophytes, vascular resurrection plants, and vegetative propogules. In: Black M, Pritchard HW (eds) Desiccation and Survival in Plants: Drying Without Dying. CABI Publishing, New York, pp 207–238

Proctor MCF, Smirnoff N (2000) Rapid recovery of photosystems on rewetting desiccation-tolerant mosses: chlorophyll fluorescence and inhibitor experiments. J Exp Bot 51: 1695–1704

Richardt S, Timmerhaus G, Lang D, Qudeimat E, Correa LG, Reski R, Rensing SA, Frank W (2010) Microarray analysis of the moss *Physcomitrella patens* reveals evolutionarily conserved transcriptional regulation of salt stress and abscisic acid signalling. Plant Mol Biol 72: 27–45

Roberts AW, Dimos CS, Budziszek MJJ, Goss CA, Lai V (2011) Knocking out the wall: protocols for gene targeting in *Physcomitrella patens*. Methods Mol Biol 715: 273–290

Rockland LB (1960) Saturated salt solutions for static control of relative humidity between 5° and 40° C. Anal Chem 32: 1375–1376

Schaefer DG, Zrÿd JP (1997) Efficient gene targeting in the moss *Physcomitrella patens*. Plant J 11: 1195–1206

Schindelin J, Arganda-Carreras I, Frise E, Kaynig V, Longair M, Pietzsch T, Preibisch S, Rueden C, Saalfeld S, Schmid B, Tinevez JY, White DJ, Hartenstein V, Eliceiri K, Tomancak P, Cardona A (2012) Fiji: an open-source platform for biological-image analysis. Nat Methods 9: 676–682

Schonbeck MW, Bewley JD (1981) Responses of the moss *Tortula ruralis* to desiccation treatments. II. Variations in desiccation tolerance. Can J Bot 59: 2707–2712

Shinde S, Nurul Islam M, Ng CK (2012) Dehydration stress-induced oscillations in LEA protein transcripts involves abscisic acid in the moss, *Physcomitrella patens*. New Phytol 195: 321–328

Shinde S, Shinde R, Downey F, Ng CKY (2013) Abiotic stress-induced oscillations in steady-state transcript levels of group 3 LEA protein genes in the moss, *Physcomitrella patens*. Plant Signal Behav 8: e22535

Shinozaki K, Yamaguchi-Shinozaki K (1997) Gene expression and signal transduction in water-stress response. Plant Physiol 115: 327–334

Stark LR (2017) Ecology of desiccation tolerance in bryophytes: a conceptual framework and methodology. Bryologist 120: 130–165

Takezawa D, Watanabe N, Ghosh TK, Saruhashi M, Suzuki A, Ishiyama K, Somemiya S, Kobayashi M, Sakata Y (2015) Epoxycarotenoid-mediated synthesis of abscisic acid in *Physcomitrella patens* implicating conserved mechanisms for acclimation to hyperosmosis in embryophytes. New Phytol 206: 209–219

Toldi O, Tuba Z, Scott P (2009) Vegetative desiccation tolerance: is it a goldmine for bioengineering crops? Plant Sci 176: 187–199

Wang X, Kuang T, He Y (2010) Conservation between higher plants and the moss *Physcomitrella patens* in response to the phytohormone abscisic acid: a proteomics analysis. BMC Plant Biol 10: 192

Wang X, Liu Y, Yang P (2012) Proteomic studies of the abiotic stresses response in model moss – *Physcomitrella patens*. Front Plant Sci 3: 258

Wang XQ, Yang PF, Liu Z, Liu WZ, Hu Y, Chen H, Kuang TY, Pei ZM, Shen SH, He YK (2009) Exploring the mechanism of *Physcomitrella patens* desiccation tolerance through a proteomic strategy. Plant Physiol 149: 1739–1750

Winston PW, Bates DH (1960) Saturated solutions for the control of humidity in biological research. Ecology 41: 232–237

Wood AJ (2007) Invited essay: new Frontiers in bryology and lichenology: the nature and distribution of vegetative desiccation-tolerance in hornworts, liverworts and mosses. Bryologist 110: 163–177

Xiao L, Yobi A, Koster KL, He Y, Oliver MJ (2018) Desiccation tolerance in *Physcomitrella patens*: rate of dehydration and the involvement of endogenous ABA. Plant Cell Environ 41: 275–284

Yobi A, Schlauch KA, Tillett RL, Yim WC, Espinoza C, Wone BW, Cushman JC, Oliver MJ (2017) *Sporobolus stapfianus*: insights into desiccation tolerance in the resurrection grasses from linking transcriptomics to metabolomics. BMC Plant Biol 17: 67

Yotsui I, Saruhashi M, Kawato T, Taji T, Hayashi T, Quatrano RS, Sakata Y (2013) ABSCISIC ACID INSENSITIVE3 regulates abscisic acid-responsive gene expression with the nuclear factor Y complex through the ACTT-core element in *Physcomitrella patens*. New Phytol 199: 101–109

Zhang F, Han M, Lv Q, Bao F, He Y (2015) Identification and expression profile analysis of NUCLEAR FACTOR-Y families in *Physcomitrella patens*. Front Plant Sci 6: 642–642

Supporting Information

Additional supporting information may be found online in the Supporting Information section at the end of the article.

Table S1. List of primers used in this study.

Fig. S1. Protonemata survival after desiccation.

Fig. S2. Gametophore survival after desiccation.

Fig. S3. Map of the *PTaEM::CFP::35s* construct.

Fig. S4. Polymerase chain reaction validation of *PTaEM::CFP::35s DNA* cassette in selected moss lines.

Fig. S5. Brightfield image of moss protonemata after acclimation.

Fig. S6. CFP localization in gametophore bud by confocal microscopy.

Edited by R. Mittler